

# Pulsed plasma deposition of chromium oxide/chromium-cermet coatings

D. Gall, R. Gampp,<sup>a)</sup> H. P. Lang, and P. Oelhafen

University of Basel, Institute of Physics, Klingelbergstrasse 82, CH-4056 Basel, Switzerland

(Received 9 October 1995; accepted 8 December 1995)

A novel radio frequency magnetron sputtering method for the deposition of composite films which consist of chromium oxide and chromium ( $\text{Cr}_2\text{O}_3/\text{Cr}$ -cermet) is presented. As an extension to conventional reactive sputtering of a Cr target in an argon and oxygen atmosphere the oxygen flow into the process chamber is switched periodically on and off. This leads to an oscillating oxygen partial pressure during the sputtering process and an alternating deposition of metallic chromium and chromium oxide. *In situ* x-ray and ultraviolet photoelectron spectroscopy are used to monitor the oxidation state of chromium at the film surface and to study the chemical interactions between adjacent layers. *Ex situ* x-ray diffraction analysis reveals the multilayered and nanocrystalline structure of the deposited films. The overall chromium and chromium oxide concentration is estimated from the optical constants  $n$  and  $k$  determined by reflectance and transmission measurements in the wavelength range between 400 and 2200 nm. © 1996 American Vacuum Society.

## I. INTRODUCTION

$\text{Cr}_2\text{O}_3/\text{Cr}$ -cermet coatings are commercially used for optically selective surfaces of solar collectors.<sup>1-3</sup> Usually, these coatings are electroplated on metal substrates and form in combination with the substrate a solar selective absorber. Compared to electroplating, however, sputtering is more environmentally sound with less pollution of the environment.

An obvious sputter deposition method for the production of  $\text{Cr}_2\text{O}_3/\text{Cr}$ -cermets is the reactive sputtering of a chromium target in an argon and oxygen atmosphere. It is expected that the deposited film consists of a mixture of metallic chromium and chromium oxide because oxidation takes place on the target, on the substrate and in the gas phase. Thereby a suitable choice of the process parameters, especially oxygen and argon flow, should lead to a desired film stoichiometry. However, many case studies in the literature have revealed that a monotonous increase of the oxygen flow results in an unsteady change of the deposition process. At a critical value of oxygen flow the deposition rate shows a sharp drop<sup>4-7</sup> and the deposited material passes abruptly from a metal to a dielectric.<sup>7</sup> This was explained by the poisoning of the target; in other words the complete coverage of the target with an oxide layer, and the subsequent change in sputtering yield.<sup>4-7</sup> The deposition of substoichiometric oxides or dielectric-metal mixtures with conventional reactive sputtering is therefore a highly critical task.<sup>7</sup>

In our own first experiments the transition behavior has been confirmed in the chromium-oxygen system. We observed a switching of the plasma color when increasing the oxygen flow from below to above the critical oxygen flow. At low oxygen flow the deposited films consisted of mainly metallic chromium and the plasma color was blue, at high oxygen flow the films were almost completely oxidized and the plasma color was reddish. The switching of the plasma

color is related to the reduction of plasma emission lines from chromium atoms<sup>8</sup> and is a consequence of the decrease in sputtering rate.

In this paper a novel rf magnetron sputtering method for the deposition of composite coatings of  $\text{Cr}_2\text{O}_3$  and Cr is described. By switching alternately between the two plasma modes below and above the critical oxygen flow, metallic Cr and chromium oxide are deposited alternately resulting in a multilayered film. The switching was done by a pulsed inlet of oxygen gas. The experimental setup as well as first investigations of the properties of these multilayered  $\text{Cr}_2\text{O}_3/\text{Cr}$  films will be presented.

## II. EXPERIMENT

A schematic drawing of the deposition chamber is shown in Fig. 1. The principal components are two electrodes facing each other in a vertical parallel plate configuration. One electrode is the chromium target (90 mm diameter) mounted on a water-cooled magnetron while the other electrode is the substrate holder. The magnetron is capacitively coupled via an impedance matching network to the rf power supply (13.56 MHz) and the substrate is grounded.

During sputtering the process gas inlet is controlled as shown in Fig. 2. While argon steadily flows into the chamber, the oxygen inlet is switched by valve 1 and valve 2. During the oxygen-on period valve 1 is open and valve 2 is closed and a constant flow of oxygen is fed into the chamber. In the oxygen-off period valve 1 is closed and valve 2 is open. Then the oxygen flow from the controller is directed to a rotary pump and the oxygen within the deposition chamber is pumped down by the throttled pumping system. Synchronous with some seconds delay to the switching of the valves, the plasma changed color. This visualized the operation of the target in the poisoned and not-poisoned mode. The  $\text{O}_2$  partial pressure in the chamber was determined by a differentially pumped mass spectrometer (Leybold-Heraeus Quadrovac Q200).

<sup>a)</sup>Author to whom correspondence should be addressed. Electronic mail: gampp@urz.unibas.ch

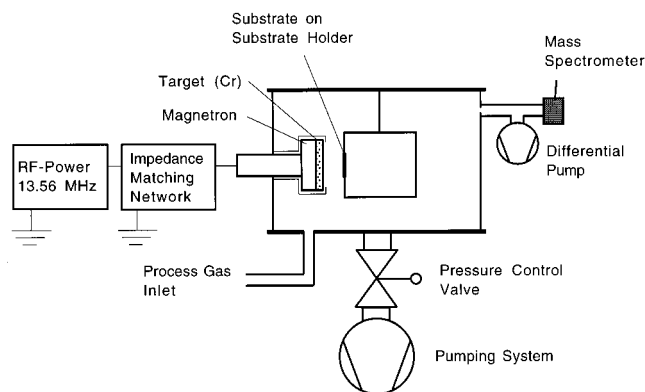


FIG. 1. Experimental setup of the deposition chamber.

In order to get more information about the chemical interaction between adjacent layers produced in each period of the pulsed plasma deposition, an interface experiment was performed: Fractions of a chromium layer were deposited step by step onto a chromium oxide layer and analyzed by *in situ* photoelectron spectroscopy.

The further parameters of the pulsed plasma deposition and the interface experiment are summarized in Table I.

After deposition, films were transferred *in situ* into the photoelectron spectrometer (Leybold EA10/100) which is equipped for ultraviolet photoelectron spectroscopy (UPS) and x-ray photoelectron spectroscopy (XPS). The photon energies used were  $h\nu = 21.22$  eV (He I mode of a discharge resonance lamp) and  $h\nu = 1253.6$  eV (Mg  $K\alpha$  radiation). Depending on the analyzer operation mode and the linewidth of the excitation radiation, an energy resolution of 0.2 eV in UPS and 1.0 eV in XPS has been obtained. The core line binding energies were calibrated by measuring Au or Pd reference samples, assuming a binding energy of 84.0 eV for the Au  $4f_{7/2}$  or 335.2 eV for the Pd  $3d_{5/2}$  core line, respectively.

A thick film which was deposited on glass (sample S2) was characterized by *ex situ* bulk analysis methods: x-ray

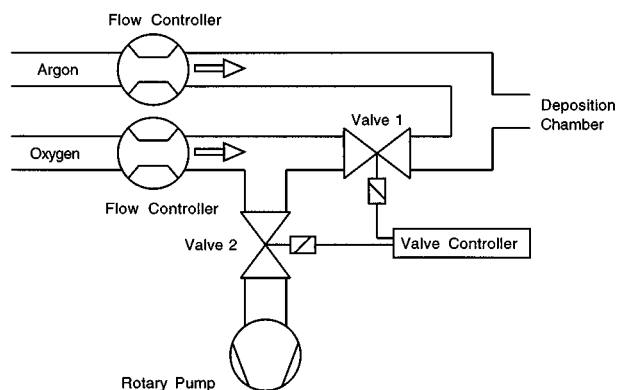


FIG. 2. Schematic drawing of the process gas inlet.

TABLE I. Deposition parameters.

	Pulsed plasma deposition	Interface experiment
Target	Cr	Cr
Target-substrate distance	90 mm	90 mm
Base pressure	$2 \times 10^{-4}$ Pa	$1 \times 10^{-4}$ Pa
Radio frequency power	200 W	50 W
Working pressure	$8.9 \times 10^{-1}$ Pa	$8.9 \times 10^{-1}$ Pa
Ar flow	40 sccm	40 sccm
O <sub>2</sub> flow	2 sccm	2 sccm (chromium oxide) 0 sccm (chromium)
Oxygen-on period	5 s (S1) 2.5 s (S2)	...
Oxygen-off period	10 s	...
Target self-bias	430 V	167 V
Substrate	Si wafer (S1) AF45 glass (S2)	Si wafer
Deposition rate	2 Å/s	0.2 Å/s

diffraction ( $\theta-2\theta$  diffractometer from Siemens, x-ray source: Cu  $K\alpha$ ) and transmission and reflectance measurements at different angles of incidence and polarizations in the wavelength range between 400 and 2200 nm (Varian CARY 5 spectrophotometer). For the optical analysis a model of a homogenous film on a thick substrate was assumed. To calculate the extended Fresnel formula for transmission and reflectance of the sample, consequently, multiple reflections in the film were added coherently and those in the substrate incoherently.<sup>9</sup> We determined the refractive index  $n$  and extinction coefficient  $k$  of the film by a least square fit of these formulas to the measured data (a detailed description of the fitting procedure is given elsewhere<sup>10</sup>).

### III. RESULTS AND DISCUSSION

#### A. Chromium/chromium oxide interface

The reaction and mixing between adjacent chromium and chromium oxide layers were analyzed in an interface experiment. For this purpose we first deposited a chromium oxide layer by reactive sputtering. The color of the plasma during the deposition was reddish. Onto this layer pure chromium was reactively sputtered in sequential steps and the surface of the resulting films was analyzed by *in situ* XPS and UPS. At each step chromium with an equivalent thickness of about 2 Å, as estimated by microbalance measurements, was deposited. The XPS spectra of the Cr  $2p_{3/2}$  core level taken from the pure chromium oxide film and after each chromium deposition cycle are displayed in Fig. 3. Vertical lines indicate binding energies of crystalline chromium oxides [CrO<sub>3</sub> (Ref. 11), CrO<sub>2</sub> (Ref. 12), Cr<sub>2</sub>O<sub>3</sub> (Refs. 12 and 13)] and metallic chromium.<sup>14</sup> It should be noted that the Cr  $2p_{3/2}$  binding energy does not monotonously change with oxidation state. This has been discussed previously.<sup>12</sup> The spectrum at the bottom of Fig. 3 corresponds to the initially deposited chromium oxide film. It consists of two peaks: A

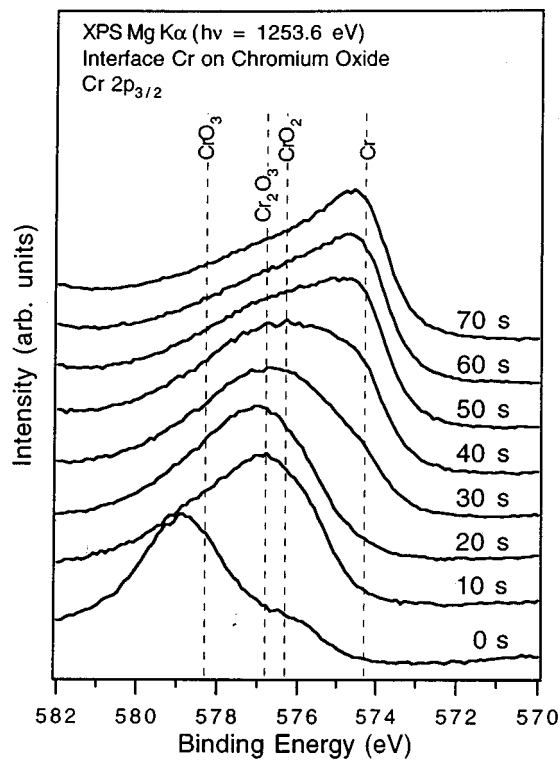


FIG. 3. XPS Cr  $2p_{3/2}$  core level spectrum of the reactively sputtered chromium oxide film and spectra taken after the indicated chromium deposition time. (For clarity the spectra are normalized to the same peak height and are shifted on the intensity scale.)

main peak situated at a binding energy of about 578.8 eV and a secondary peak at about 576.0 eV. These peaks are assigned to two different oxidation states of chromium: Cr<sup>6+</sup> at the higher binding energy close to the position of the crystalline CrO<sub>3</sub> reference and Cr<sup>4+</sup> close to the CrO<sub>2</sub> reference.

The surface of the film was drastically modified after 10 s chromium deposition.<sup>15</sup> The maximum of the Cr  $2p_{3/2}$  peak is now situated between the positions of the crystalline oxides Cr<sub>2</sub>O<sub>3</sub> and CrO<sub>2</sub> and the peak shape indicates that both oxidation states, Cr<sup>3+</sup> and Cr<sup>4+</sup> are present at the film surface. Obviously, all newly deposited chromium atoms were oxidized by the underlying chromium oxide layer. No Cr<sup>6+</sup> is observable within the depth sensitivity of the XPS analysis which is estimated to be about 10 Å.<sup>16</sup> After 20 s chromium deposition the Cr  $2p_{3/2}$  signal is dominated by a single peak at about 577.0 eV, which corresponds to an oxidation state of Cr<sup>3+</sup> as in the crystal Cr<sub>2</sub>O<sub>3</sub>. After about 30 s chromium deposition, metallic chromium with a Cr  $2p_{3/2}$  binding energy of about 574.3 eV is present at the film surface. The chromium which is deposited in the next steps covers the underlying Cr<sub>2</sub>O<sub>3</sub> and hence the peak which corresponds to metallic chromium increases and the Cr<sub>2</sub>O<sub>3</sub> signal decreases. After about 70 s chromium deposition time the spectra do not change any more. The chromium layer has grown to a thickness at which essentially all photoelectrons originate from it. Therefore, these spectra reflect the properties of bulk rf sputtered chromium.

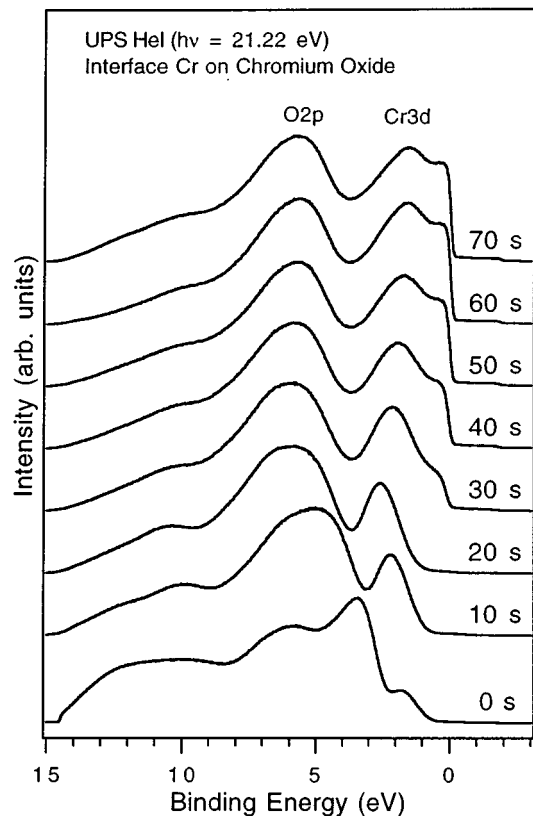


FIG. 4. UPS He I valence band spectra of film surfaces as in Fig. 3.

The He I valence band spectrum of the reactively sputtered chromium oxide film and spectra taken after the indicated chromium deposition times are shown in Fig. 4. The spectrum of the chromium oxide film (bottom spectrum) is dominated by three peaks at binding energies of about 1.5, 3.5, and 6.0 eV. The small peak at 1.5 eV is assigned to Cr 3d electrons and the other two peaks to O 2p electrons according to the high oxidation state of this film. After 10 and 20 s chromium deposition the relative intensity of the Cr 3d peak increased. This is in agreement with the interpretation of a decreasing oxidation state of chromium at the film surface derived from the XPS spectra. Furthermore, the splitting of the O 2p peaks becomes smaller and all peaks are shifted to higher binding energy. The weak feature near 10 eV binding energy has been assigned to a multielectron satellite in the case of pure Cr<sub>2</sub>O<sub>3</sub>.<sup>17</sup> The He I valence band spectrum after 20 s chromium deposition is very similar to the spectrum of crystalline Cr<sub>2</sub>O<sub>3</sub>.<sup>18</sup> After 30 s chromium deposition a Fermi edge characteristic for metallic materials develops. Up to about 60 s chromium deposition time the portion of chromium 3d states below the Fermi energy increases, whereupon the spectra are almost identical. These findings indicate metallic chromium after 30 s deposition time and the successive growth of a metallic chromium layer in accordance with the analysis of the XPS spectra.

It can be concluded from the interface experiment that in the reddish mode of the plasma almost completely oxidized chromium with an oxidation state close to Cr<sup>6+</sup> is deposited.

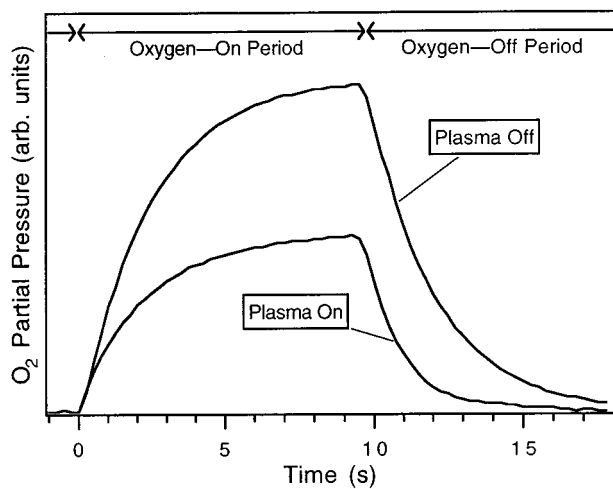


FIG. 5. O<sub>2</sub> partial pressure in the deposition chamber during an oxygen-on and an oxygen-off period. The upper curve results from measurement without plasma, the lower curve from measurement with the plasma glowing.

If pure chromium is sputtered onto this chromium oxide film the film surface is reduced finally to Cr<sup>3+</sup> before the deposited chromium grows in metallic form.

### B. Partial pressure measurements

Figure 5 shows the change of the O<sub>2</sub> partial pressure during an oxygen-on and an oxygen-off period. The upper curve belongs to a measurement at switched off rf power, i.e., without plasma. The characteristic time  $\tau$  for increase and decrease of the partial pressure as well as its saturation value is determined by chamber volume, pumping speed, and flow of oxygen. According to a numerical estimation  $\tau$  is about 2 s which is close to the experimental value. The lower curve shows the O<sub>2</sub> partial pressure during the deposition with the plasma glowing. The O<sub>2</sub> partial pressure during the plasma process is always lower than without plasma. This can be explained by an increased pumping speed resulting from gettering of oxygen by continuously deposited chromium.

### C. Pulsed plasma deposition

Various samples have been deposited by repeated oxygen-on and oxygen-off cycles. In the case of sample S1 the deposition was interrupted three times in order to analyze the sample surface. The *in situ* photoelectron spectroscopy measurements were performed (A) at the end of the oxygen-on period (5 s interval), (B) in the middle, and (C) at the end of the oxygen-off period (10 s interval). The corresponding Cr 2p<sub>3/2</sub> core level spectra are shown in Fig. 6.

The Cr 2p<sub>3/2</sub> core level of sample A is similar to the spectrum taken from the chromium oxide film after 20 s chromium deposition in the interface experiment (see Fig. 3). Within the depth sensitivity of the XPS analysis chromium with an oxidation state of Cr<sup>3+</sup> dominates. Regarding the distinct O 2p splitting and the Cr 3d position in the He I spectrum in Fig. 7 an even higher oxidation state must be

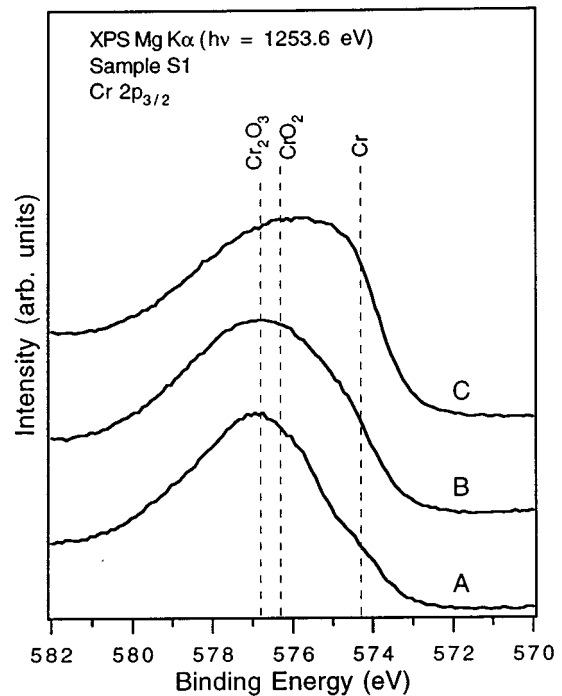


FIG. 6. XPS Cr 2p<sub>3/2</sub> core level spectra recorded from the surface of a film which was deposited by the pulsed plasma method (sample S1). The deposition cycles were interrupted for the measurements at three different moments: (A) after 5 s sputtering in the oxygen-on period, (B) after 5 s sputtering in the oxygen-off period, and (C) after 10 s sputtering in the oxygen-off period.

present within the UPS photoelectron escape depth. These findings reflect that after the oxygen-on period, a chromium oxide layer has formed on the film surface. After 5 s deposition in the oxygen-off period, both the Cr 2p<sub>3/2</sub> spectrum (curve B in Fig. 6) and the He I spectrum (curve B in Fig. 7) indicate metallic chromium at the sample surface. Obviously time was sufficient to pump down the oxygen partial pressure, to sputter clean the target and to reduce the sample surface. After 10 s deposition in the oxygen-off period (curve C in Figs. 6 and 7) the portion of metallic chromium at the sample surface has further increased.

The photoelectron spectroscopy measurements clearly show the oscillation of the oxidation state of Cr at the surface of a growing film during the pulsed plasma deposition. However, these measurements cannot provide direct information about the overall chromium and oxygen concentration of the resulting films.

### D. X-ray diffraction (XRD)

An XRD measurement of sample S2 is shown in Fig. 8. No further background subtraction was applied except for removing the scattered intensity from the glass substrate. Above about  $2\theta = 25^\circ$  the spectrum shows broad structures typical of amorphous and nanocrystalline materials. The wide maximum at  $2\theta = 36^\circ$  corresponds to a next neighbor

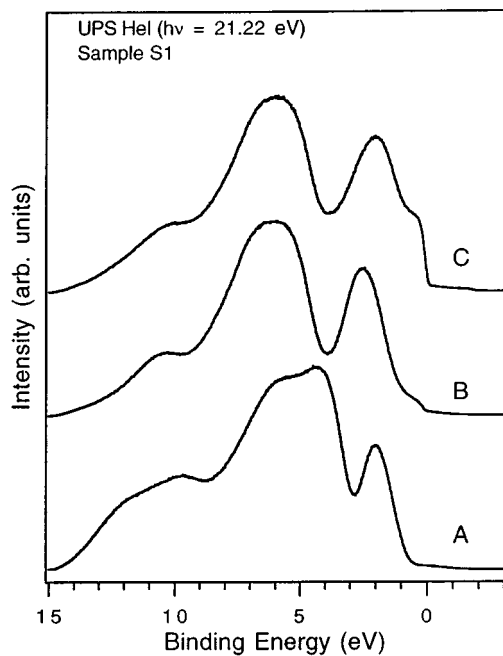


FIG. 7. UPS He I valence band spectra of film surfaces as in Fig. 6.

distance of about  $2.5 \text{ \AA}$  comparable to the distance between the closest packed (110) planes in crystalline  $\text{Cr}_2\text{O}_3$  [ $2.48 \text{ \AA}$  (Ref. 19)].

At  $2\theta = 3.58^\circ$  and  $2\theta = 7.01^\circ$  sharp peaks are observed. They are first and second order diffraction maxima resulting from the regular layer sequence of the film. In real space these maxima correspond to a distance of  $24.6 \text{ \AA}$  between equivalent layers. From that length and the total number of deposition cycles a film thickness of  $473 \text{ nm}$  is inferred.

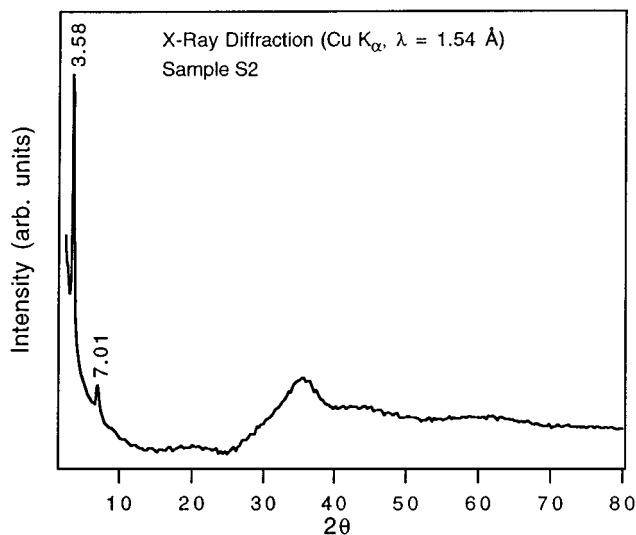


FIG. 8. X-ray diffraction spectrum of sample S2. The contribution of the glass substrate has been subtracted.

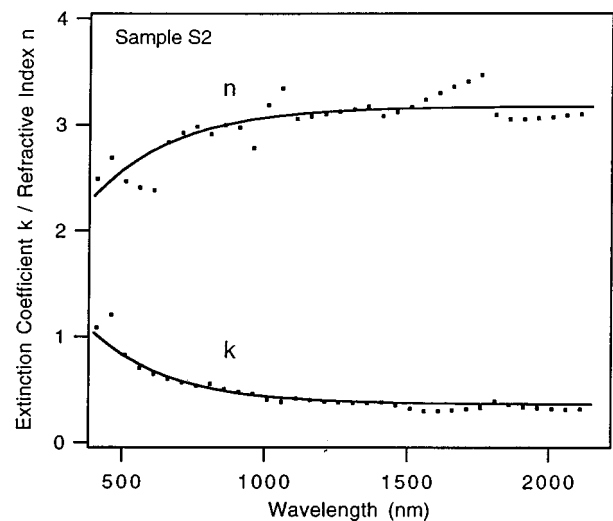


FIG. 9. Refractive index  $n$  and extinction coefficient  $k$  of sample S2. The solid line corresponds to a curve fit and the data points to a fit in which the  $n$  and  $k$  values were calculated for each wavelength separately.

### E. Optical constants

The layer-by-layer thicknesses in the film are small compared to wavelengths in the visible and infrared region. For those wavelengths, the film appears as homogenous and the optical behavior can be described with effective optical constants. The refractive index  $n$  and the extinction coefficient  $k$  of sample S2 are drawn as a function of wavelength in Fig. 9. For their evaluation the film thickness as determined by XRD has been used. The data points result from a fitting procedure which determines at each wavelength  $n$  and  $k$  values. In addition  $n$  and  $k$  were modeled by exponential curves  $y(\lambda) = a + b \exp(-c\lambda)$ . In this case the coefficients were optimized over the whole wavelength range. The resulting curves are drawn as solid lines and may serve as a guide to the eye.

The optical constants  $n$  and  $k$  may be compared to data published by Fan and Spura.<sup>20,21</sup> They analyzed  $\text{Cr}_2\text{O}_3/\text{Cr}$ -cermet films of different composition which were deposited by co-sputtering of a Cr and a  $\text{Cr}_2\text{O}_3$  target. If we assume a chromium concentration of  $26 \pm 2 \text{ vol. \%}$  for our film, our and their optical constants match in the absolute values (see especially Fig. 8 in Ref. 21) and in the wavelength dependency. The increase of  $n$  as well as the decrease of  $k$  from lower to higher wavelengths is well reproduced.

### IV. CONCLUSION

A new method for the deposition of  $\text{Cr}_2\text{O}_3/\text{Cr}$ -cermet coatings has been presented. By switching on and off the oxygen flow during the rf sputtering of a Cr target, chromium and chromium oxide are deposited alternately and a multilayered film results. The distance between equivalent layers was determined by XRD and amounts to about  $25 \text{ \AA}$ . An intense intermixing of adjacent layers was found by *in situ* photoelectron spectroscopy measurements. The refrac-

tive index  $n$  and extinction coefficient  $k$  of the composite film were evaluated by transmission and reflectance measurements. This made possible the estimation of the overall composition. A film with  $26 \pm 2$  vol. % Cr was deposited which would have been very difficult with conventional reactive sputtering. However, further investigations are necessary in order to determine the total accessible range of concentration and the suitability for solar selective applications.

## ACKNOWLEDGMENTS

This work was financially supported by the Swiss Bundesamt für Energiewirtschaft under Grant No. EF-REN(92)075. We are indebted to A. Helmbold who wrote the computer program for the determination of the optical constants and to C. Hague for the careful reading of the manuscript.

<sup>1</sup>C. M. Lampert and J. Washburn, *Sol. Energy Mater.* **1**, 81 (1979).

<sup>2</sup>M. G. Hutchins, *Surf. Technol.* **20**, 301 (1983).

<sup>3</sup>C. G. Granqvist, *Appl. Phys. A* **52**, 83 (1991).

<sup>4</sup>J. Heller, *Thin Solid Films* **17**, 163 (1973).

<sup>5</sup>T. Abe and T. Yamashina, *Thin Solid Films* **30**, 19 (1975).

<sup>6</sup>S. Maniv and W. D. Westwood, *J. Appl. Phys.* **51**, 718 (1980).

<sup>7</sup>J. A. Thornton, in *Deposition Technologies for Films and Coatings*, edited by R. F. Bunshah (Noyes, Park Ridge, NJ, 1982), p. 170.

<sup>8</sup>W. Graf (private communication).

<sup>9</sup>E. Elizalde and F. Rueda, *Thin Solid Films* **122**, 45 (1984).

<sup>10</sup>A. Helmbold, Ph.D. thesis, University of Hannover, Hannover, Germany, 1993.

<sup>11</sup>G. C. Allen, M. T. Curtis, A. J. Hooper, and P. M. Tucker, *J. Chem. Soc. Dalton Trans.* 1675 (1973).

<sup>12</sup>I. Ikemoto *et al.*, *J. Solid State Chem.* **17**, 425 (1976).

<sup>13</sup>E. Paparazzo, *Surf. Interface Anal.* **12**, 115 (1988).

<sup>14</sup>C. D. Wagner, W. M. Riggs, L. E. Davis, J. F. Moulder, and G. E. Muilenberg, *Handbook of X-ray Photoelectron Spectroscopy* (Perkin-Elmer, Eden Prairie, MN, 1979).

<sup>15</sup>Immediately before the deposition of each chromium layer the Cr target was cleaned in a pure Ar plasma. Thereby oxygen which has accumulated on the target surface was removed. This cleaning procedure was particularly necessary after the reactive sputtering of the chromium oxide layer since the Cr target was oxidized.

<sup>16</sup>M. P. Seah and W. A. Dench, *Surf. Interface Anal.* **1**, 2 (1979).

<sup>17</sup>D. E. Eastman and J. L. Freeouf, *Phys. Rev. Lett.* **34**, 395 (1975).

<sup>18</sup>G. K. Wertheim, H. J. Guggenheim, and S. Hüfner, *Phys. Rev. Lett.* **30**, 1050 (1973).

<sup>19</sup>International Center of Powder Diffraction Data (ICPDS), *Powder Diffraction File* (ICPDS, Newtown Square, PA, 1994).

<sup>20</sup>J. C. C. Fan and S. A. Spura, *Appl. Phys. Lett.* **30**, 511 (1977).

<sup>21</sup>J. C. C. Fan, *Thin Solid Films* **54**, 139 (1978).